

Electronic Structure of (6–4) DNA Photoproduct Repair Involving a Non-Oxetane Pathway

Tatiana Domratcheva* and Ilme Schlichting

Department of Biomolecular Mechanisms, Max Planck Institute for Medical Research, Jahnstrasse 29, 69120 Heidelberg, Germany

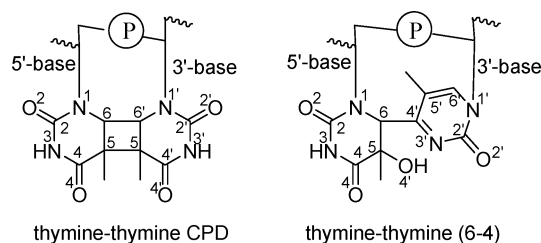
Received June 4, 2009; E-mail: Tatjana.Domratcheva@mpimf-heidelberg.mpg.de

Abstract: Mutagenic pyrimidine–pyrimidone (6–4) photoproducts are one of the main DNA lesions induced by solar UV radiation. These lesions can be photoreversed by (6–4) photolyases. The originally published repair mechanism involves rearrangement of the lesion into an oxetane intermediate upon binding to the (6–4) photolyase, followed by light-induced electron transfer from the reduced flavin cofactor. In a recent crystallographic study on a (6–4) photoproduct complexed with (6–4) photolyase from *Drosophila melanogaster* no oxetane was observed, raising the possibility of a non-oxetane repair mechanism. Using quantum-chemical calculations we find that in addition to repair via an oxetane, a direct transfer of the hydroxyl group results in reversal of the radical anion (6–4) photoproduct. In both mechanisms, the transition states have high energies and correspond to avoided crossings of the ground and excited electronic states. To study whether the repair can proceed via these state crossings, the excited-state potential energy curves were computed. The radical excitation energies and accessibility of the nonadiabatic repair path were found to depend on hydrogen bonds and the protonation state of the lesion. On the basis of the energy calculations, a nonadiabatic repair of the excited (6–4) lesion radical anion via hydroxyl transfer is probable. This repair mechanism is in line with the recent structural data on the (6–4) photolyase from *D. melanogaster*.

Introduction

Solar radiation is a DNA damaging agent that can introduce covalent bonds between adjacent pyrimidine bases. The two major forms of DNA damage, cyclobutane pyrimidine dimers (CPD) and pyrimidine–pyrimidone (6–4) photoproducts, are mutagenic and often carcinogenic.^{1–4} The chemical structures of these lesions and their atom numbering are shown in Chart 1. In many organisms these photoproducts can be repaired or “photoreactivated” by light-dependent flavoenzymes known as photolyases. Two types of photolyases have been discovered: the CPD photolyase⁵ capable of repairing CPD lesions and the (6–4) photolyase⁶ specific for (6–4) photoproducts. Both photolyases utilize flavin adenine nucleotide (FAD) in its two-electron reduced anionic form as a redox cofactor. Reactivation of CPDs by the photolyase has been studied in great detail (reviewed in refs 7–12). At the catalytic site, the lesion is bound in close proximity to the FAD cofactor. The CPD photolyase uses light energy to transfer an electron from the excited reduced flavin to the bound lesion. The reduced anionic CPD radical

Chart 1. DNA Photolesions



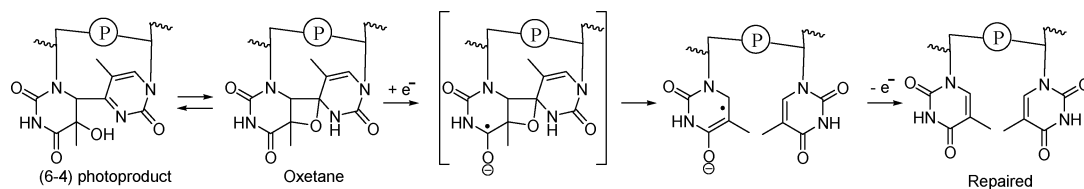
undergoes spontaneous cycloreversion into a pair of parental nucleotides. The enzymatic cycle is concluded by electron transfer from the repaired bases back to the flavin cofactor, restoring its initial redox state.

In contrast, much less is known about DNA repair by the (6–4) photolyase, currently a subject of intensive study.^{8,13–17} The (6–4) photolyase specifically binds to sites that contain (6–4) lesions and, upon photon absorption, catalyzes the repair

- (1) Taylor, J. S. *Pure Appl. Chem.* **1995**, *67*, 183–190.
- (2) Kamiya, H.; Iwai, S.; Kasai, H. *Nucleic Acids Res.* **1998**, *26*, 2611–2617.
- (3) Matsumura, Y.; Ananthaswamy, H. N. *Front. Biosci.* **2002**, *7*, d765–d783.
- (4) Reardon, J. T.; Sancar, A. *Genes Dev.* **2003**, *17*, 2539–2551.
- (5) Rupert, C. S.; Goodgal, S. H.; Herriott, R. M. *J. Gen. Physiol.* **1958**, *41*, 451–471.
- (6) Todo, T.; Takemori, H.; Ryo, H.; Ihara, M.; Matsunaga, T.; Nikaido, O.; Sato, K.; Nomura, T. *Nature* **1993**, *361*, 371–374.
- (7) Sancar, A. *Chem. Rev.* **2003**, *103*, 2203–2237.
- (8) Sancar, A. *J. Biol. Chem.* **2008**, *283*, 32153–32157.
- (9) Heelis, P. F.; Hartman, R. F.; Rose, S. D. *Chem. Soc. Rev.* **1995**, *24*, 289–297.

- (10) Carell, T.; Burgdorf, L. T.; Kundu, L. M.; Cichon, M. *Curr. Opin. Chem. Biol.* **2001**, *5*, 491–498.
- (11) Weber, S. *Biochim. Biophys. Acta* **2005**, *1707*, 1–23.
- (12) Essen, L. O.; Klar, T. *Cell. Mol. Life Sci.* **2006**, *63*, 1266–1277.
- (13) Hitomi, K.; DiTacchio, L.; Arvai, A. S.; Yamamoto, J.; Kim, S. T.; Todo, T.; Tainer, J. A.; Iwai, S.; Panda, S.; Getzoff, E. D. *Proc. Natl. Acad. Sci. U.S.A.* **2009**, *106*, 6962–6967.
- (14) Muller, M.; Carell, T. *Curr. Opin. Struct. Biol.* **2009**, *19*, 277–285.
- (15) Glas, A. F.; Maul, M. J.; Cryle, M.; Barends, T. R. M.; Schneider, S.; Kaya, E.; Schlichting, I.; Carell, T. *Proc. Natl. Acad. Sci. U.S.A.* **2009**, *106*, 11540–11545.
- (16) Glas, A. F.; Schneider, S.; Maul, M. J.; Hennecke, U.; Carell, T. *Chem.—Eur. J.* **2009**, *15*, 10387–10396.
- (17) Yamamoto, J.; Hitomi, K.; Hayashi, R.; Getzoff, E. D.; Iwai, S. *Biochemistry* **2009**, *48*, 9306–9312.

Scheme 1. (6-4) Photoproduct Repair via an Oxetane Intermediate



reaction.^{6,18–20} Despite the different chemical structures of the lesions, a common repair mechanism was suggested on the basis of high sequence homology between the CPD and (6–4) photolyases.^{18,19} Photorepair of the (6–4) photoproduct was proposed to proceed via a four-membered ring oxetane intermediate, which is formed from a ring-closing isomerization of the (6–4) photoproduct catalyzed by the photolyase. Photoreduction of the oxetane results in repair in a similar fashion as in the case of CPDs. The enzymatic repair of the thymine–thymine (6–4) dimer involving an oxetane intermediate is shown in Scheme 1. The oxetane intermediate is formed by a proton transfer from O4'H to N3'. In the case of the thymine–cytosine (6–4) dimer, the four-membered ring azetidone intermediate (not shown) can be formed and split in a similar manner to oxetane.

An oxetane is a presumed intermediate in the DNA photo-damage reaction following the Paterno–Büchi (2 + 2) cycloaddition of the C6=C5 and C4'=O4' double bonds in two adjacent thymine bases.^{21–24} At temperatures exceeding $-80\text{ }^{\circ}\text{C}$, the oxetane intermediate undergoes rapid isomerization to afford the (6–4) photoproduct²² via a mechanism that is poorly understood. In contrast, the sulfur analogue of oxetane, a thietane, was reported to be stable and to interconvert with the corresponding (6–4) form.²⁵ Irradiation of the thietane reversed it into the parent nucleotides.^{26,27} However, synthetic thietane DNA lesions were not repaired by (6–4) photolyase.¹⁹ Nonetheless, it was proposed that the (6–4) photolyase can stabilize an oxetane or azetidone by a mechanism involving two conserved histidine residues.²⁸ Enzyme-assisted isomerization of the (6–4) dimer into an oxetane was proposed to consist of two proton transfer steps: from O4'H to the first neutral (deprotonated) histidine and from the second cationic (protonated) histidine to N3'.²⁹ This mechanism is consistent with the observed H/D isotope effect and pH dependence of the enzymatic repair,²⁸ mutational studies,²⁸ and results of electron paramagnetic resonance (EPR)/electron–nuclear double resonance (ENDOR) experiments that established the protonation states of the histidines without the lesion bound.²⁹ The oxetane formed may undergo cycloreversion in a photoreductive process with FAD

as an electron donor, followed by electron transfer back to the flavin. The reductive cycloreversion reaction has been demonstrated for a number of model oxetane compounds, providing supporting evidence for the oxetane-repair model.^{30,31}

The electronic structure and energies of the reductive and oxidative oxetane cycloreversion have been studied by quantum-chemical methods.^{32–34} Comparison of the oxidative and reductive mechanisms of the (6–4) photolyase in terms of energetics indicated that an oxidative process is favorable and that the oxetane is split in the radical anion form.³⁴ In the thymine–thymine oxetane radical anion, the C5–O4' bond breaks spontaneously and the C6–C4' bond cleavage requires only a small activation energy.^{32,34} A similar mechanism was proposed for the thymine–cytosine azetidone with a somewhat higher activation energy.^{32,34} Taken together, the theoretical and experimental studies convincingly demonstrated that an oxetane can be repaired along the reductive radical pathway. However, there is no evidence that an oxetane is indeed formed during the (6–4) photolyase reaction.

Recently, the crystal structure of the (6–4) photolyase from *Drosophila melanogaster* bound to a DNA duplex containing a thymine–thymine (6–4) photoproduct was determined.³⁵ The (6–4) lesion was found in the binding pocket without being rearranged to an oxetane. The orientation and interactions of the two conserved histidine residues are at odds with oxetane formation, and there is no other residue interacting with the lesion in a manner to promote oxetane generation. Strikingly, upon flavin reduction and light illumination of the crystals, the (6–4) lesion was successfully repaired *in situ*.³⁵ Therefore, the new structural data question the popular oxetane repair model and evoke the possibility of a non-oxetane repair mechanism.

In our study, quantum-chemical calculations were used to characterize the electronic structure of the thymine–thymine (6–4) dimer and its repair reaction in the radical anion state. Two major topics were addressed: (i) the energy and mechanism of the oxetane formation in the radical anion state and (ii) the existence of a non-oxetane repair reaction. The results demonstrate that the (6–4) photoproduct radical anion is a rather stable chemical species and that its repair via oxetane and non-oxetane pathways requires significant activation energies. The non-oxetane reaction, reported here for the first time, proceeds via hydroxyl transfer and yields the repaired 3'-base in the enol tautomeric form. The hydroxyl transfer is associated with the crossing of the ground and excited electronic states, suggesting

(18) Kim, S. T.; Malhotra, K.; Smith, C. A.; Taylor, J. S.; Sancar, A. *J. Biol. Chem.* **1994**, *269*, 8535–8540.

(19) Zhao, X.; Liu, J.; Hsu, D. S.; Zhao, S.; Taylor, J. S.; Sancar, A. *J. Biol. Chem.* **1997**, *272*, 32580–32590.

(20) Mizukoshi, T.; Hitomi, K.; Todo, T.; Iwai, S. *J. Am. Chem. Soc.* **1998**, *120*, 10634–10642.

(21) Varghese, A. J.; Wang, S. Y. *Science* **1968**, *160*, 186–187.

(22) Rahn, R. O.; Hosszu, J. L. *Photochem. Photobiol.* **1969**, *10*, 131–137.

(23) Asgatay, S.; Petermann, C.; Harakat, D.; Guillaume, D.; Taylor, J. S.; Clivio, P. *J. Am. Chem. Soc.* **2008**, *130*, 12618–12619.

(24) Blancafort, L.; Migani, A. *J. Am. Chem. Soc.* **2007**, *129*, 14540–14541.

(25) Clivio, P.; Fourrey, J. L.; Gasche, J.; Favre, A. *J. Am. Chem. Soc.* **1991**, *113*, 5481–5483.

(26) Clivio, P.; Fourrey, J. L. *Chem. Commun.* **1996**, 2203–2204.

(27) Liu, J.; Taylor, J. S. *J. Am. Chem. Soc.* **1996**, *118*, 3287–3288.

(28) Hitomi, K.; Nakamura, H.; Kim, S. T.; Mizukoshi, T.; Ishikawa, T.; Iwai, S.; Todo, T. *J. Biol. Chem.* **2001**, *276*, 10103–10109.

(29) Schleicher, E.; Hitomi, K.; Kay, C. W.; Getzoff, E. D.; Todo, T.; Weber, S. *J. Biol. Chem.* **2007**, *282*, 4738–4747.

(30) Prakash, G.; Falvey, D. E. *J. Am. Chem. Soc.* **1995**, *117*, 11375–11376.

(31) Joseph, A.; Prakash, G.; Falvey, D. E. *J. Am. Chem. Soc.* **2000**, *122*, 11219–11225.

(32) Wang, Y.; Gaspar, P.; Taylor, J. S. *J. Am. Chem. Soc.* **2000**, *122*, 5510–5519.

(33) Izquierdo, M. A.; Domingo, L. R.; Miranda, M. A. *J. Phys. Chem. A* **2005**, *109*, 2602–2607.

(34) Borg, O. A.; Eriksson, L. A.; Durbeek, B. *J. Phys. Chem. A* **2007**, *111*, 2351–2361.

(35) Maul, M. J.; Barends, T. R.; Glas, A. F.; Cryle, M. J.; Domratcheva, T.; Schneider, S.; Schlichting, I.; Carell, T. *Angew. Chem., Int. Ed.* **2008**, *47*, 10076–10080.

a nonadiabatic process starting from the excited (6-4) radical anion. The oxetane and hydroxyl transfer repair mechanisms are discussed in the context of the biochemical and structural data on (6-4) photolyases.

Computational Methods

Quantum-chemical calculations were performed on a thymine–thymine (6-4) photoproduct via the B3LYP and UB3LYP methods for the singlet neutral and radical anion molecules, respectively. A model consisting of two N1-methylated thymine bases was used for all calculations. The starting geometry of the (6-4) lesion was constructed on the basis of coordinates of the (6-4) photolyase of *D. melanogaster* (PDB code 3cvu).³⁵ Geometries of the (6-4) and oxetane lesions were optimized. To study the repair mechanism, intrinsic reaction coordinates were computed by the Gonzalez–Schlegel second-order method.³⁶ All minima and saddle points were confirmed by computing the harmonic vibrational frequencies.

Calculations of the excited states of the radical anions were carried out by the configuration interaction singles and doubles (CISD) method with the reference Hartree–Fock singlet wave function. Single and double electron excitations were considered for a window of 14 occupied molecular orbitals (MOs) and 10 virtual MOs. For all geometries tested, the radical ground state has a predominant single-determinant character, confirming the UB3LYP results. The relative CISD energies are overestimated compared to the UB3LYP ones. However, all energetic trends in the ground state were qualitatively reproduced. The CISD calculations were used to study the state switch at the rate-determining transition states. To this end, the five lowest electronic states were computed at the geometries comprising the intrinsic reaction coordinates, starting from the highest energy saddle points.

A standard TZV basis set was used throughout the calculations. All calculations were performed with the PC GAMESS/Firefly³⁷ quantum chemistry package, which is partially based on the GAMESS (US)³⁸ source code.

Results and Discussion

The crystal structure of the (6-4) lesion bound to the (6-4) photolyase of *D. melanogaster* was determined recently (PDB code 3cvu).³⁵ The active-site pocket containing the DNA lesion is shown in Figure 1. The pyrimidine 5'-base forms numerous hydrogen bonds with the enzyme. In contrast, the pyrimidone 3'-base, including its N3' atom, does not form hydrogen bonds. The crystal structure was used to construct the starting geometry of the thymine–thymine (6-4) dimer (two N1-methylthymine bases) considered in our study. Similar models were employed in recent computational studies on DNA photodamage^{24,39,40} and photorepair.^{32,34} This model allowed us to address the electronic structure of the repair reaction.

The (6-4) photoproduct and oxetane structures were optimized in the singlet state. The vertical radical anions, that is, the species formed by electron injection without any structural change, were computed at the obtained minima. The geometries were then optimized to find the radical-anion equilibrium structures. Optimized geometries and the lowest unoccupied

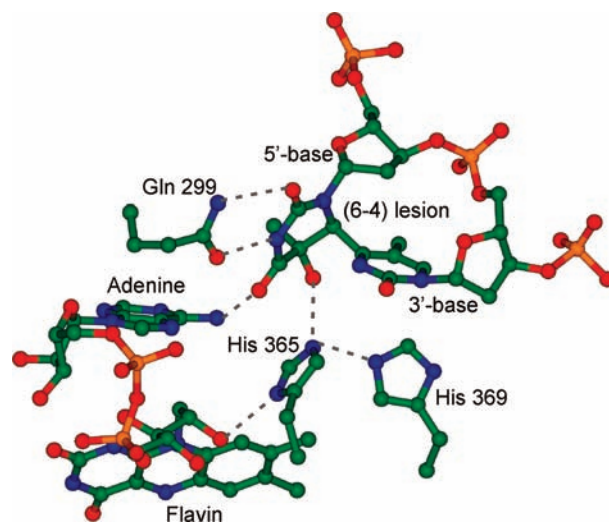


Figure 1. Binding of the thymine–thymine (6-4) lesion to the (6-4) photolyase observed in the crystal structure.³⁵ Hydrogen bonds are tentatively assigned on the basis of interatomic distances and are indicated by dashed lines.

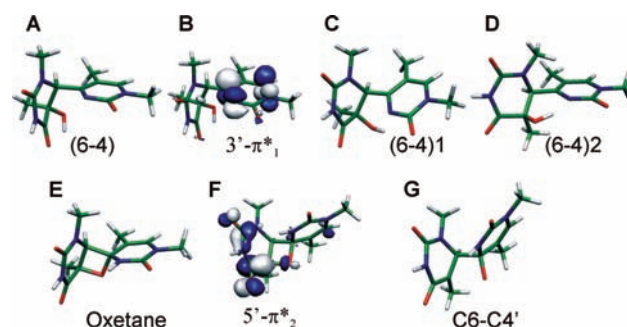


Figure 2. Optimized geometries of the singlet and radical anion (6-4) and oxetane lesions and the LUMO/SOMOs.

molecular orbitals (LUMO) are shown in Figure 2. In the singlet (6-4) photoproduct (Figure 2A), the pyrimidone 3'-base has an energetically favorable aromatic π -system. Accordingly, the LUMO is the antibonding $3'-\pi^*$ orbital of the conjugated 3'-base (Figure 2B). This orbital becomes the single occupied molecular orbital (SOMO) in the radical anion. The vertical radical anion energy is 9.1 kcal/mol lower than the energy of the singlet minimum. Upon geometry optimization, the radical anion is further stabilized by formation of a hydrogen bond between the O4'H group and the N3' atom [structure (6-4)1 in Figure 2C], compensating the negative charge localized at the 3'-base. The adiabatic electron affinity of the (6-4) lesion, calculated as a difference between the energies of singlet and radical anion minima, is 19.2 kcal/mol, indicating that the (6-4) radical anion can be stable. In contrast, the parent thymine base does not form a stable anion radical according to experiment⁴¹ and theory.^{42,43} In agreement, the UB3LYP/TZV adiabatic electron affinity of N1-methylthymine is -0.9 kcal/mol. In the course of the reaction pathway calculations, another radical anion minimum structure with a different orientation of the

(36) Gonzalez, C.; Schlegel, H. B. *J. Chem. Phys.* **1989**, *90*, 2154–2161.

(37) Granovsky, A. A. PC GAMESS/Firefly version 7.1.F, <http://classic-chem.msu.su/gran/gamess/index.html>.

(38) Schmidt, M. W.; Baldridge, K. K.; Boatz, J. A.; Elbert, S. T.; Gordon, M. S.; Jensen, J. H.; Koseki, S.; Matsunaga, N.; Nguyen, K. A.; Su, S. J.; Windus, T. L.; Dupuis, M.; Montgomery, J. A. *J. Comput. Chem.* **1993**, *14*, 1347–1363.

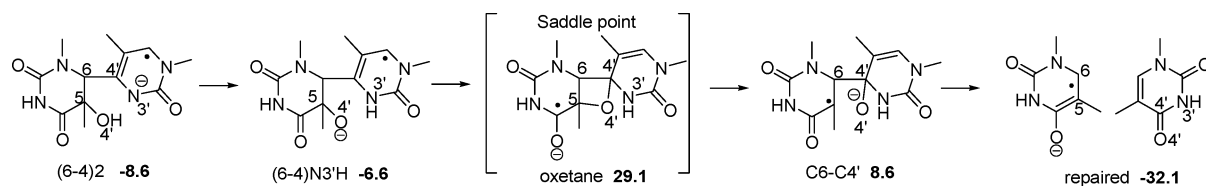
(39) Boggio-Pasqua, M.; Groenhof, G.; Schafer, L. V.; Grubmüller, H.; Robb, M. A. *J. Am. Chem. Soc.* **2007**, *129*, 10996–10997.

(40) Roca-Sanjuan, D.; Olaso-Gonzalez, G.; Gonzalez-Ramirez, I.; Serrano-Andres, L.; Merchán, M. J. *J. Am. Chem. Soc.* **2008**, *130*, 10768–10779.

(41) Desfrancois, C.; Abdoul-Carime, H.; Schermann, J. P. *J. Chem. Phys.* **1996**, *104*, 7792–7794.

(42) Desfrancois, C.; Abdoul-Carime, H.; Carles, S.; Periquet, V.; Schermann, J. P.; Smith, D. M. A.; Adamowicz, L. *J. Chem. Phys.* **1999**, *110*, 11876–11883.

(43) Sevilla, M. D.; Besler, B.; Colson, A. O. *J. Phys. Chem.* **1995**, *99*, 1060–1063.

Scheme 2. Structures and Energies along the Radical-Anion Repair Reaction Involving an Oxetane

nucleotide bases—structure (6-4)2 in Figure 2D—was found. The additional stabilization of the (6-4)2 minimum by 8.6 kcal/mol compared to the (6-4)1 minimum is provided by widening of the O4'H–N3' hydrogen bond angle from 132° in (6-4)1 to 149° in (6-4)2.

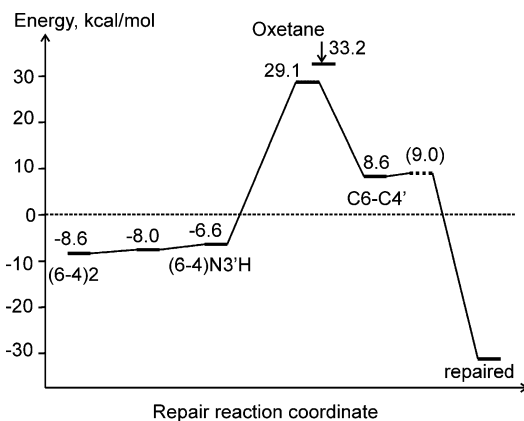
In the singlet oxetane (Figure 2E), loss of 3'-base aromatic stabilization increases the energy of the molecule by 11 kcal/mol compared to the energy of the (6-4) photoproduct. The high energy of the oxetane was presented previously as an argument against the oxetane-repair model.⁴⁴ In the oxetane geometry, the singlet state LUMO is the 5'- π^* orbital of the carbonyl groups in the pyrimidine 5'-base (Figure 2F). The vertical radical anion of the oxetane is 4.3 kcal/mol higher in energy than the oxetane singlet minimum. Upon geometry relaxation, spontaneous splitting of the C5–O4' bond affords the C6–C4' intermediate (Figure 2G), whose energy is 20.6 kcal/mol lower than the energy of the oxetane singlet minimum. The spontaneous cycloreversion of the oxetane upon reduction, which forms the cornerstone of the oxetane-repair model, has been established in previous computational studies.^{32,34}

The (6-4) lesion repair consists of three steps including dissociation of the C5–O4' bond, formation of the O4'–C4' bond, and dissociation of the C6–C4' bond. The energy scans along the respective intrinsic coordinates were obtained, starting from the (6-4)1 anion radical geometry. High-energy transition states corresponding to O4'–C4' bond formation and C5–O4' bond dissociation but not to C6–C4' bond dissociation were found. Increasing the C6–C4' bond distance in the (6-4)1 anion radical increases the energy significantly and does not result in any stable product. Therefore, the (6-4) lesion radical anion does not fragment into modified bases, in agreement with repair experiments and previous calculations for the oxetane model.³⁴ From the two transition states, intrinsic reaction coordinate calculations were performed. Complete pathways were identified that represent two repair reactions. The relative energies of the stationary points of these pathways were computed with respect to the reference energy of the (6-4)1 radical anion presented in Figure 2C and account for zero-point vibrations.

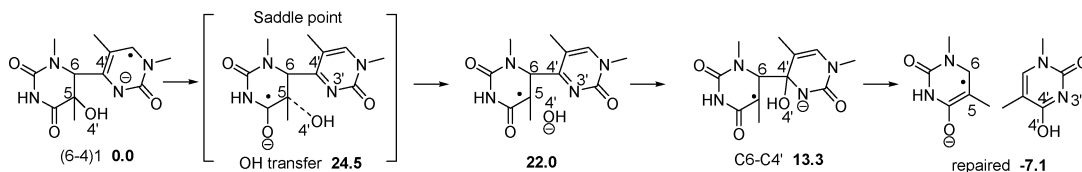
The first pathway includes a transition state with the oxetane structure. Scheme 2 presents the structures of the stationary points; Figure 3 shows the energy diagram where stationary points are indicated by their relative energies. The reference energy corresponding to the (6-4)1 radical anion is indicated as a dashed zero line in Figure 3. The reaction starts from the (6-4)2 radical anion minimum (−8.6 kcal/mol). Before the O4'–C4' bond is formed, the proton is transferred to N3'. The respective proton transfer transition state was found. After correction for zero-point vibrational energy, its energy (−8.0 kcal/mol) was smaller than the energy of the (6-4)N3'H minimum (−6.6 kcal/mol), rendering the latter structure unstable. It is important to note that a hydrogen bond and proton transfer to the N3' nitrogen atom decreases the energy of the (6-4) radical anion and increase the oxetane activation energy.

At the oxetane transition state (29.1 kcal/mol), the C4'–O4' bond distance is 1.75 Å, which is longer than the corresponding 1.54 Å distance in the oxetane singlet minimum. The C4'–O4' stretching imaginary frequency is 618i cm^{−1}. The vertical oxetane radical (33.2 kcal/mol), indicated in Figure 3 by an arrow, corresponds to the energy at which the cycloreversion starts when the singlet oxetane is formed and reduced, that is, the pathway addressed by the previous computational studies.^{32,34} The unstable intermediate C6–C4' (8.6 kcal/mol) was introduced earlier in Figure 2G. No saddle point could be localized that connects the C6–C4' and the repaired minima. The restrained energy optimization revealed that the transition state is situated very close to the C6–C4' intermediate and its energy does not exceed 9 kcal/mol, which corresponds to an activation energy of less than 0.5 kcal/mol. Accounting for zero-point vibrational energy could further decrease this value. Therefore, in agreement with the previous studies, our reaction coordinate calculations suggest that the oxetane radical is spontaneously converted to the repaired structure. In addition, we found that rearrangement of the (6-4) radical anion to the oxetane form requires high activation energy.

Along the second pathway, repair proceeds via transfer of the O4'H hydroxyl group from the 5'-base to the 3'-base. This is a novel pathway and its implications for the enzymatic repair were not discussed previously in the literature. Changes in structure and energy taking place along this pathway are presented in Scheme 3 and Figure 4, respectively. The hydroxyl transfer repair starts from the (6-4)1 minimum (0.0 kcal/mol). The stabilizing O4'H–N3' hydrogen bond is disrupted on the way to the hydroxyl transfer rate-determining transition state, prior to C5–O4' bond dissociation. The vertical (6-4) radical anion (10.1 kcal/mol), indicated by an arrow, does not have this hydrogen bond. Accordingly, its structure is situated somewhat closer to the transition state and its repair requires less activation energy. As in oxetane repair, the O4'H–N3' hydrogen bond stabilizes the 3'-base radical and has an anticatalytic effect on repair. The highest-energy transition state (24.5 kcal/mol) corresponds to dissociation of the C5–O4' bond.

**Figure 3.** Energy profile of oxetane repair. The dotted zero line corresponds to the energy of the (6-4)1 radical anion presented in Figure 2C.(44) Heelis, P. F.; Liu, S. B. *J. Am. Chem. Soc.* **1997**, *119*, 2936–2937.

Scheme 3. Structures and Energies along the Radical-Anion Repair Pathway Involving Hydroxyl Transfer



At the saddle point geometry, the C5–O4' distance is 1.83 Å and the C5–O4' stretching imaginary frequency is 540i cm⁻¹. A shallow minimum (22.0 kcal/mol) corresponds to a structure with the dissociated hydroxyl fragment in the van der Waals contact with the methyl group of the 3'-base. The O4'–C4' bond formation results in the C6–C4' intermediate (13.3 kcal/mol), which is the enol form of the C6–C4' intermediate (8.6 kcal/mol) of the oxetane pathway. Dissociation of the C6–C4' bond in the former structure requires 0.5 kcal/mol activation energy. The repaired structure, concluding the hydroxyl transfer pathway, contains the enol tautomer of the 3'-base.

The reaction pathway calculations demonstrate that (6-4) repair via oxetane and hydroxyl transfer can be regarded as reactions with a single energy barrier related to either formation of the C4'–O4' bond or dissociation of the C5–O4' bond, respectively. These critical energy barriers are rather high, whereas all other computed energy barriers are negligibly small. Thus, the (6-4) radical is stable and might be observable experimentally. Significant activation energy is required, rendering the repair along these two pathways a rather slow process. In the photolyase, these slow repair reactions cannot compete with the fast electron transfer back to the flavin.

The oxetane and hydroxyl transfer transition states correspond to a radical anion with the SOMO localized on the 5'-base, whereas in the (6-4) form the SOMO is on the 3'-base. This state switch is demonstrated by the 3'-π*₁ and 5'-π*₂ molecular orbitals in Figure 2, panels B and F, respectively, for the oxetane case. Therefore, in terms of the electronic structure, the repair is achieved via populating the 5'-π*₂ base radical, which can be split practically without activation. In Schemes 2 and 3, the 3'- and 5'-base radicals are indicated by location of the radical dot. From the (6-4) form to the critical transition state, the radical is localized on the 3'-π*₁ orbital, whereas thereafter, it is on the 5'-π*₂ orbital. The 3'-π*₁/5'-π*₂ radical state switch is related to the crossing of the electronic states and indicates a possible photochemical reaction that involves a nonadiabatic path starting from the excited state instead of climbing up the high energy barrier. Since the enzymatic repair is a photoreaction, a nonadiabatic process is conceivable that starts from the excited radical anion and overcomes the oxetane or hydroxyl transfer energy barriers.

To test a possible nonadiabatic repair mechanism, the excited radical anions were characterized by the CISD method. The

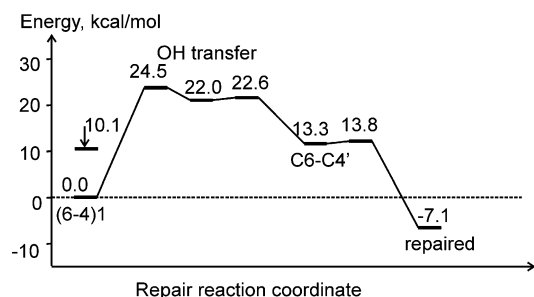


Figure 4. Energy profile of the hydroxyl transfer repair pathway.

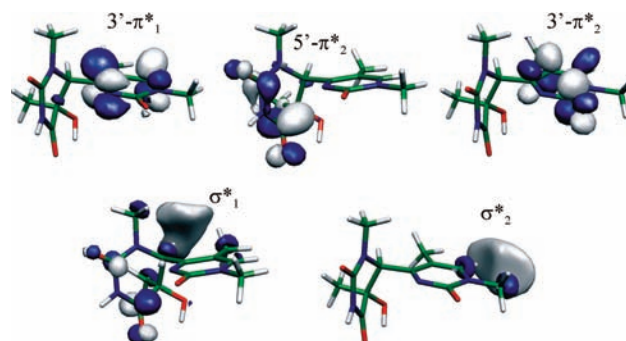


Figure 5. The (6-4) radical anion SOMO in the ground and excited states.

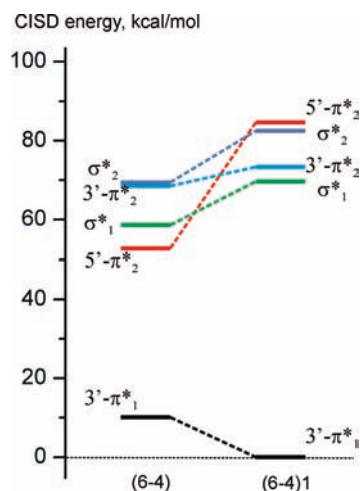


Figure 6. Electron excitation energies of the (6-4) photoproduct radical anion at the (6-4) and (6-4)1 geometries presented in Figure 2, panels A and C, respectively.

energies and wave functions of the five lowest electronic states were computed at the geometries along the reaction coordinates. For all geometries discussed below, these electronic states have a predominant single-determinant character and can be assigned to single-electron excitations of the unpaired electron in either the π* or the σ* orbitals shown in Figure 5. Population of the π* orbitals corresponds to thymine valence radicals. Population of the σ* orbitals represents electron attachment,^{42,45} that is, a singlet lesion interacting with an electron in a diffuse orbital. The CISD electron excitation spectra of the (6-4) radical anion at the (6-4) singlet and (6-4)1 radical anion geometries are shown in Figure 6. There are clear differences in the electronic structure upon radical stabilization by the O4'H–N3 hydrogen bond. In addition to decreasing the energy of the 3'-π*₁ ground state, as already indicated by the UB3LYP calculations, the hydrogen bond significantly increases the energy of the 5'-π*₂ excited state. Reordering of the electronic states by the

(45) Desfrancois, C.; Abdoul-Carime, H.; Schulz, C. P.; Schermann, J. P. *Science* **1995**, *269*, 1707–1709.

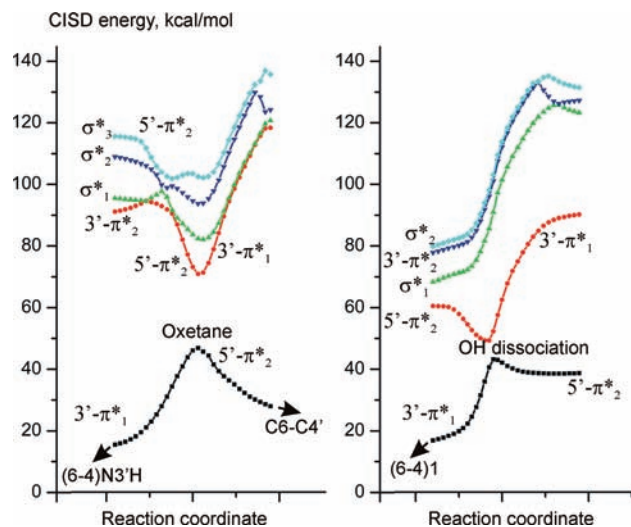


Figure 7. Energy diagram illustrating avoided crossings along the repair coordinates for the oxetane (left) and hydroxyl transfer (right) pathways.

O4'H–N3 hydrogen bond or N3' protonation is an important feature of the (6–4) lesion radical.

Figure 7 illustrates the computed energy curves supplemented with the state assignments. The left panel shows the formation of the C4'–O4' bond via oxetane; the right panel shows dissociation of the C5–O4' bond via hydroxyl release. To allow a direct comparison, the CISD energies were computed with respect to the same reference: the CISD energy of the (6–4)1 radical anion in the ground state. As anticipated, the oxetane formation and hydroxyl dissociation transition states correspond to the $3'-\pi^*_1/5'-\pi^*_2$ avoided crossings. As shown in the left panel of Figure 7, complex changes of the electronic structure involving multiple state crossings occur upon oxetane formation. In the (6–4)N3'H structure, preceding C4'–O4' bond formation, the $3'-\pi^*_2$ state is the first excited state, whereas the energy of the $5'-\pi^*_2$ state is very high. Formation of the C4'–O4' bond disrupts the π -conjugation in the 3'-base, and the energies of the $3'-\pi^*_1$ and the $3'-\pi^*_2$ states increase. Concomitantly, the energy of the $5'-\pi^*_2$ state decreases upon approaching the oxetane geometry. The $3'-\pi^*_2/5'-\pi^*_2$ crossing and the $3'-\pi^*_1/5'-\pi^*_2$ avoided crossing were found along the oxetane reaction path.

For the hydroxyl transfer shown in the right panel of Figure 7, the N3' nitrogen atom remains unprotonated and the energy of the $5'-\pi^*_2$ state is lowered significantly, enabling it to be the first excited state at the geometries preceding the transition state. In that case, the $3'-\pi^*_1/5'-\pi^*_2$ state crossing may be accessible for the (6–4) lesion radical excited to the $5'-\pi^*_2$ state. Upon C5–O4' bond dissociation, the $5'-\pi^*_2$ state energy decreases and the $3'-\pi^*_1$ state energy increases in the same manner as in the oxetane, which ultimately results in the $3'-\pi^*_1/5'-\pi^*_2$ avoided crossing. The energy gap of the avoided crossing is rather small, indicating a close conical intersection. It is suggestive that the (6–4) radical anion excited to the $5'-\pi^*_2$ state may use this conical intersection as relaxation path and undergo nonadiabatic repair reaction.

In the crystal structure of the *D. melanogaster* (6–4) photolyase bound to the (6–4) lesion, no oxetane formation was observed and the determined positions of the two conserved histidines are incompatible with the proposed oxetane formation. Therefore, it has been suggested that the (6–4) lesion, without being rearranged to the oxetane, accepts an electron from the

flavin and the formed (6–4) radical anion undergoes repair.³⁵ In our quantum-chemical study we show that the (6–4) radical anion with unpaired electron localized on the pyrimidone 3'-base is energetically favorable and can be further stabilized by the intramolecular hydrogen bond. The oxetane formation is accomplished by a proton transfer, mediated by the O4'H–N3' intermolecular hydrogen bond, followed by C4'–O4' bond formation. The latter step, with high activation energy, cannot compete with the fast electron transfer back to the flavin in the photolyase. A nonadiabatic repair via the oxetane state crossing is also unlikely because of the stabilization of the $3'-\pi^*_1$ radical and the destabilization of the $5'-\pi^*_2$ radical upon N3' protonation, as the energy diagram in Figure 7 illustrates. Therefore, we conclude that the oxetane repair pathway, starting from the (6–4) lesion radical anion, is not feasible. Currently, it cannot be excluded that small amounts of oxetane, undetectable in a crystallographic study, could be formed in the singlet state and split in a photoreduction reaction. The mechanism of the oxetane formation, which is different from the originally proposed histidine-assisted mechanism, remains to be clarified. Critical for the oxetane repair, protonation of the N3' nitrogen atom might be mediated by the O4'H–N3' intermolecular hydrogen bond that was proposed to exist in the singlet (6–4) lesion in solution on the basis of spectroscopic studies.^{46,47}

Stabilization of the 3'-radical anion of the (6–4) photoproduct by hydrogen-bonding interactions would be unfavorable for the repair reaction and, in fact, no such hydrogen bonds could be proposed on the basis of the crystal structure.³⁵ We also note that a general acid situated in the vicinity of the 3'-pyrimidone ring should also result in anticatalytic stabilization of the 3'-base radical. The same effect should be expected for a chemically modified (6–4) lesion containing a positively charged 3'-base. The enzymatic repair of the modified (6–4) photoproduct containing a NH_2^+ iminium cation instead of the C2'=O2' carbonyl in the 3'-base has been recently studied. The stability of this imine analogue in the enzymatic repair was attributed to the role of the C2'=O2' carbonyl group in the enzymatic repair reaction.¹⁷ Formation of the stable 3'-base radical, which the (6–4) photolyase cannot repair, might be another explanation prompted by our electronic structure study.

The hydroxyl transfer represents an alternative repair pathway. As our calculations suggest, the activation energy of the hydroxyl transfer can be decreased in an environment where the (6–4) radical anion cannot form a stabilizing intramolecular O4'H–N3 hydrogen bond. In line with this, the crystal structure of the *D. melanogaster* photolyase³⁵ suggests a hydrogen bond between the O4'H hydroxyl group and the conserved histidine 365. When the N3' atom is deprotonated and the stabilizing O4'H–N3' hydrogen bond cannot form, the excited $5'-\pi^*_2$ radical anion of the (6–4) lesion may undergo a nonadiabatic repair via hydroxyl transfer. This mechanism implies that light-induced electron transfer from the flavin yields the excited (6–4) photoproduct radical anion. As shown in Figure 7, the energy of the (6–4) form in the excited $5'-\pi^*_2$ state only slightly exceeds the energy of the oxetane radical anion. It is also conceivable that the hydrogen bonds between the pyrimidine 5'-base and the photolyase identified in the crystal structure decrease the energy of the excited $5'-\pi^*_2$ radical state.

(46) Yamamoto, J.; Tanaka, Y.; Hitomi, K.; Getzoff, E. D.; Iwai, S. *Nucleic Acids Symp. Ser.* **2007**, 79–80.

(47) Yamamoto, J.; Tanaka, Y.; Iwai, S. *Org. Biomol. Chem.* **2009**, 7, 161–166.

In conclusion, our calculations demonstrate that the (6-4) photoproduct has a high positive electron affinity and its radical anion with unpaired electron localized in the pyrimidone 3'-base is a stable species. In the electronic ground state, its reversal to the parent nucleotides proceeds via high-energy transition states. The two characterized repair pathways involve either the previously suggested oxetane formation or a novel hydroxyl transfer. Notably, both repair reactions involve conversion of a stable 3'-base radical into an unstable 5'-base radical. Along the hydroxyl transfer pathway, a nonadiabatic relaxation of the excited 5'-base radical can result in repair. Accessibility of this relaxation path critically depends on hydrogen bonds and the protonation state of N3'. The highly specific hydrogen-bonding interactions with the lesion may enable the hydroxyl transfer constituting the key contribution of the (6-4) photolyase. Further calculations on an extended molecular system including the electron donor and accounting for specific hydrogen-bonding

interactions in the active site of the (6-4) photolyase are necessary to demonstrate the exact role of the hydrogen bonds and evaluate the hydroxyl transfer as a possible enzymatic repair mechanism.

Acknowledgment. We gratefully acknowledge Chris Roome for excellent support of the computational hardware and software; Thomas R. M. Barends and Max J. Cryle for helpful discussions and suggestions; Thomas Carell and his group (LMU Munich) for a fruitful collaboration; and the Deutsche Forschungsgemeinschaft (DFG) for financial support through SFB749.

Supporting Information Available: Cartesian coordinates, absolute energies, and other characteristics of the stationary points. This material is available free of charge via the Internet: <http://pubs.acs.org>.

JA904550D